



Pollution characteristics, sources, and health risk assessments of urban road dust in Kuala Lumpur City

Murnira Othman^{1,2} · Mohd Talib Latif¹

Received: 11 October 2019 / Accepted: 2 January 2020
© Springer-Verlag GmbH Germany, part of Springer Nature 2020

Abstract

Urban road dust contains anthropogenic components at toxic concentrations which can be hazardous to human health. A total of 36 road dust samples from five different urban areas, a commercial (CM), a high traffic (HT), a park (GR), a rail station (LRT), and a residential area (RD), were collected in Kuala Lumpur City followed by investigation into compositions, sources, and human health risks. The concentrations of trace metals in road dust and the bioaccessible fraction were determined using inductively couple plasma-mass spectrometry (ICP-MS) while ion concentrations were determined using ion chromatography (IC). The trace metal concentrations were dominated by Fe and Al with contributions of 53% and 21% to the total trace metal and ion concentrations in road dust. Another dominant metal was Zn while the dominant ion was Ca^{2+} with average concentrations of $314 \pm 190 \mu\text{g g}^{-1}$ and $3470 \pm 1693 \mu\text{g g}^{-1}$, respectively. The most bioaccessible fraction was Zn followed by the sequence $\text{Sr} > \text{Cd} > \text{Cr} > \text{Cu} > \text{Ni} > \text{Co} > \text{Mn} > \text{As} > \text{V} > \text{Pb} > \text{Fe} > \text{Al} > \text{U}$. The results revealed that the highest trace metal and ion concentrations in road dust and in the bioaccessible fraction were found at the LRT area. Based on the source apportionment analysis, the major source of road dust was vehicle emissions/traffic activity (47%), and for the bioaccessible fraction, the major source was soil dust (50%). For the health risk assessments, hazard quotient (HQ) and cancer risk (CR) values for each element were < 1 and in the tolerable range ($1.0\text{E-}06$ to $1.0\text{E-}04$), except for As for the ingestion pathway. This result suggests a low risk from non-carcinogenic and probable risk from carcinogenic elements, with higher health risks for children compared to adults.

Keywords Road dust · Source apportionment · Health risk assessment · Bioaccessibility · Chemical composition

Introduction

Urban areas are synonymous with the rapid development of economic activities, dense populations, and high amounts of air pollution. Air pollution released from industrial and vehicle activities coupled with other sources such as biological inputs, soil, construction materials, and biomass burning

settles to the earth's surface forming hazardous particles (Li et al. 2017; Amjadian et al. 2018; Othman et al. 2019). Solid particles with sizes $< 500 \mu\text{m}$ that settle out of the atmosphere form dust with sizes ranging between 1 and $10000 \mu\text{m}$ (Khpalwak et al. 2019; Othman et al. 2019). Dust is easily resuspended by air movements and meteorological wind patterns (Tian et al. 2018). Dust that finally settles in the environment and onto an impervious road or pavement is referred to as road dust. As road dust has a wide range of components, compositions, sizes, and properties, the main characteristics of road dust need to be explored.

Road dust is a mixture of organic matter, elemental carbon, vehicle and industrial exhaust, industrial particles, particles from residential fossil fuel burning, lubricant oil particles, and tyre-, brake- and engine-wear components as well as soil, plant and biogenic materials (Okorie et al. 2012; Kastury et al. 2017; Li et al. 2017). Road dust, especially in urban areas, is an agglomerate of multiple contributions where any anthropogenic or biogenic source of urban atmosphere can contribute to road dust composition (Liu et al. 2007). Some studies have

Responsible editor: Philippe Garrigues

Electronic supplementary material The online version of this article (<https://doi.org/10.1007/s11356-020-07633-7>) contains supplementary material, which is available to authorized users.

✉ Murnira Othman
mumira@ukm.edu.my

¹ Centre for Earth Sciences and Environment, Faculty of Science and Technology, Universiti Kebangsaan Malaysia, 43600 Bangi, Selangor, Malaysia

² Institute for Environment and Development (LESTARI), Universiti Kebangsaan Malaysia, 43600 Bangi, Selangor, Malaysia

found major contributions from vehicle and traffic activities to the chemical properties of road dust (Han et al. 2007; Liu et al. 2007; Duong and Lee 2011; Li et al. 2018). Other components in road dust such as microplastics and microrubber were also determined by Abbasi et al. (2019) who found an average of 900 microplastic and 250 microrubber particles in a 15 g dust sample, with various colors and sizes derived from a multitude of domestic, vehicular, and industrial sources.

Usually, metal contamination is the chemical property of road dust most discussed. Road dust is a sink for pollution, particularly heavy metals (Men et al. 2018). Heavy metals in road dust have been identified as the main pollution species in areas such as mining areas (Tang et al. 2017), an e-waste recycling area (Leung et al. 2008), and industrial areas (Kong et al. 2011; Urrutia-Goyes et al. 2018). However, due to the impact of growing numbers of vehicles and the increases in pollution from vehicle exhaust, metals in urban road dust have been used as indicators of heavy metal pollution in the environment (Li et al. 2001; Duong and Lee 2011). As reported by Duong and Lee (2011), the road surface materials greatly contribute to heavy metal concentrations in road dust: dust from asphalt highways is greatly impacted by vehicle exhaust; dust from concrete highways is highly affected by tyre abrasion due to the much rougher surface. Metals such as Zn and Pb are usually related to automobile emissions and industrial combustions and also white pigment on the road surface (Han et al. 2007; Dehghani et al. 2017), while metals such as Ni have been suggested to be sourced from its applications in electroplating and from nickel-cadmium batteries (Kabadayi and Cesur 2010). Hg originates from contamination from chlor-alkali production and the application of Hg cathodes in industry (Zheng et al. 2010) and Cr and Co have been thought to be sourced from alloying additives and machinery industries (Han et al. 2017; Li et al. 2018).

Other chemical compositions of road dust consist of inorganic ions, major elements, and organic matter as well as a mineralogy aspect. Ionic compositions of road dust are particularly dominated by Ca^{2+} , SO_4^{2-} , Cl^- , NO_3^- , and K^+ with sources from construction activities, secondary gas-to-particle conversion, chemical industrial emissions, and vehicle emissions (Han et al. 2007). The composition of road dust has been identified as dominated by major elements especially in commercial areas where contributions from construction work and quarries were the main sources (Ramírez et al. 2018). Other studies determined component concentrations and properties of road dust including polycyclic aromatic hydrocarbons (PAH) (Liu et al. 2007; Amjadian et al. 2018; Khanal et al. 2018; Khpalwak et al. 2019), dissolution characteristics (Joshi et al. 2009), mineralogical and morphological aspects (Gunawardana et al. 2012; Amjadian et al. 2018; Valido et al. 2018), and elemental and organic carbon (Shi et al. 2011; Ramírez et al. 2018). Overall, studies have shown higher levels of metal compositions in urban road dust compared to other areas, which can significantly impact the health of the urban population.

Humans are exposed to road dust chemical properties via three main routes: ingestion, dermal/skin absorption, and inhalation. The health risks to human health of non-carcinogenic and carcinogenic elements contained in road dust have been widely studied (Hu et al. 2011; Shi et al. 2011; Liu et al. 2014; Ali et al. 2017; Khanal et al. 2018; Li et al. 2018; Men et al. 2018). Metals such as As are carcinogenic and may affect human health in ways such as skin irritation, cardiovascular diseases, and metabolic disorders (Liu et al. 2016). Other than that, the bioaccessible fraction and its impact via human oral ingestion are becoming an important consideration in order to calculate accurate exposures of non-carcinogenic and carcinogenic elements to humans. Bioaccessibility is a test that is usually performed to indicate the metal fraction that can be mobilized from the ingested dust into the digestive juices in the gastric environment and therefore becomes bioaccessible (Leung et al. 2008; Valido et al. 2018). As reported by Luo et al. (2012) and Padoan et al. (2017), the bioaccessibility of metal pollutants is an important aspect when studying trace metals in urban environments, especially to evaluate human health risks of exposure to metals. Thus, the application of bioaccessibility assessments to assess human health risks is crucial, especially for studies related to urban pollution.

Urban road dust comprises a high amount of toxic materials that risk human health; hence, the chemical characteristics and bioaccessibility of road dust need to be investigated particularly the metals that are highly potentially toxic to human health. Urbanization, industrialization, rapid population growth, and high number of vehicles are associated with the acceleration of heavy metal contamination in urban soil and road dust in the city Kuala Lumpur (Han et al. 2013). This study aims to determine and compare the chemical composition of road dust and the bioaccessible fraction in different urban areas in Kuala Lumpur City. To identify the possible sources of trace metals and ions in road dust, positive matrix factorization (PMF) coupled with multiple linear regression (MLR) was applied. Health risk assessments of different pathways were performed which provides information regarding the potential risks associated with road dust and significantly helps in understanding the health risks of exposure to trace metals at two stages of human life, child and adult.

Materials and method

Study area

Kuala Lumpur is located on Peninsular Malaysia at 20 to 200 m above mean sea level (DBKL 2018). The city has a total area of 243.65 km² with a total population of 1.79 million people (DOS 2018). The main industrial sectors were reported to be workshops, cement and concrete manufacture, and hotels located within the boundaries of Kuala Lumpur,

particularly in the center of the city (DOE 2018). The road network in Kuala Lumpur consists of highways and major roads with roads to the city center mainly from the southern and eastern parts of Kuala Lumpur. The average temperature and humidity in Kuala Lumpur are 29 °C and 78%, respectively.

Road dust sampling and analytical analysis

Thirty six urban road dust samples within Kuala Lumpur were collected from the 8th to 24th August 2018 from five urban areas: a commercial area (CM), a high traffic area (HT), a park area (GR), a rail station area (LRT), and a residential area (RD). The main characteristics of each sampling site are described in Table S1 while the locations of the sampling sites are shown in Figure S1. At each sampling site, around 30 to 40 g of road dust sample were collected using plastic dustpans and brushes and then transferred to polyethylene bags (Men et al. 2018; Ramírez et al. 2018). During sampling, the weather was dry with no rain events for about 3 days before the sampling date. After the sampling process, the samples were air-dried for 7 days under direct sunlight in the lab and sieved with a 63 µm nylon sieve (Retsch, Germany) (Tian et al. 2018; Othman et al. 2019). This procedure was performed to be certain that the samples have dried out completely. Prior studies used certain temperature such as 460 °C and 110 °C overnight for drying purpose (Charlesworth et al. 2003; McKenzie et al. 2008).

Each sample for each urban area underwent extraction for trace metal and ion concentration analysis. The extraction of trace metals from road dust started with the digestion of 1 g of each sample in a mixture of nitric acid and perchloric acid with a ratio of 4:1 as described by Han et al. (2013). After cooling, the sample was diluted to 100 mL with ultrapure water, filtered using Pall Acrodisc syringe filters, and stored in polyethylene bottles at 4 °C. For ions, about 0.7 g of sample was leached with 15 mL ultrapure water as followed by Jaradat et al. (2004) and Othman et al. (2019). The extracted samples were then filtered using Pall Acrodisc syringe filters and transferred to polyethylene bottles. The extractions were then stored at 4 °C before analysis.

Metal bioaccessibility was determined based on the Simple Bioaccessibility Extraction (SBET) method, as by followed Padoan et al. (2017) and USEPA (2017). The extraction of road dust was performed with 0.4 M glycine solution that was adjusted to 1.5 pH and then filtered with Pall Acrodisc syringe filters. The filtered samples were kept in polyethylene bottles and stored in 4 °C before analysis.

The concentrations of trace metals from the acid digestions and bioaccessibility extractions (Al, Fe, Pb, Zn, As, Cd, Cr, Co, Cu, Mn, Ni, U, V, Sr) were determined using inductively couple plasma-mass spectrometry (ICP-MS) (PerkinElmer Elan 9000, United States of America). Ions (Na⁺, NH₄⁺, K⁺,

Ca²⁺, F⁻, Cl⁻, Br⁻, NO₃⁻, SO₄²⁻) were determined using ion chromatography (IC) (Metrohm 850 IC Plus, Switzerland). The blank and recovery analyses were processed in same manner as samples while the accuracy of the method was verified with NIST SRM 1649a urban dust. The recovery percentages and limits of detection are listed in Table S2.

Spatial distribution of trace metals

The spatial distributions of trace metal and ion concentrations in road dust and the bioaccessible fraction were determined using spatial interpolation and GIS mapping techniques. Several spatial interpolation techniques such as inverse distance weighting (IDW), triangulated irregular network (TIN) and kriging were also tested to understand the application of each method. For this study, the ordinary kriging method was applied where kriging can express the spatial distribution and also minimize the error of the predicted values (Shi et al. 2008). ArcGIS 10.2 software (ESRI Co, United States of America) with a semi-variance function and spherical model was selected (Men et al. 2018).

Assessment of trace metal pollution

Assessment of trace metal pollution in road dust was carried out using the geoaccumulation index (*I_{geo}*), pollution index (PI), and enrichment factor (EF). As reported by Othman et al. (2019), *I_{geo}* and PI can provide the degree of pollution enrichment while Chen et al. (2014) stated that the calculation of EF can be used to differentiate anthropogenic and natural sources.

I_{geo} was calculated based on the soil background value as shown in Eq. (1) as followed by Li et al. (2011), Men et al. (2018), and Tian et al. (2018):

$$I_{geo} = \log_2 \left(\frac{C_n}{1.5B_n} \right) \quad (1)$$

where C_n is the concentration of element n in road dust and B_n is the concentration of element n taken from Taylor and McLennan (1985). The classification of *I_{geo}* values was: $I_{geo} \leq 0$ is uncontaminated, 0–1 indicates uncontaminated to moderately contaminated, 1–2 indicates moderately contaminated, 2–3 indicates moderately to strongly contaminated, 3–4 indicates strongly contaminated, 4–5 indicates strongly to extremely contaminated, and > 5 indicates extremely contaminated (Li et al. 2011).

The PI was calculated based on the ratio of metal concentrations in road dust and reference concentrations as reported in Eq. (2):

$$PI = \frac{C_n}{B_n} \tag{2}$$

where C_n is the concentration of element n in road dust and B_n is the reference concentration of element n . The reference concentrations for elements in soil were taken from Taylor and McLennan (1985). The PI values are classified as: $PI \leq 1$ is low level pollution, $1 < PI \leq 3$ is mid-level of pollution, and $PI > 3$ is high level of pollution (Faiz et al. 2009).

EF is the ratio of trace metal concentrations in the dust sample to the reference/background concentrations (Shi and Lu 2018). The calculation of EF followed Ramírez et al. (2018) and Shi and Lu et al. (2018) as in Eq. (3):

$$EF = \left(\frac{C_i}{C_{Al}} \right)_{sample} / \left(\frac{B_i}{B_{Al}} \right)_{background} \tag{3}$$

where $\frac{C_i}{C_{Al}}_{sample}$ and $\frac{B_i}{B_{Al}}_{background}$ are the ratio of the concentrations of element i and Al in road dust and the ratio of the concentrations of element i and Al in background soil. The background concentrations of trace metals were taken from Taylor and McLennan (1985). The EF values were classified based as: EF values close to 1 indicate natural origins; 1–2 indicates minimal anthropogenic sources; 2–5 indicates moderate anthropogenic sources; 5–20 indicates significant anthropogenic sources; 20–40 indicates very high anthropogenic sources; and > 40 indicates extremely high anthropogenic sources (Ramírez et al. 2018).

Source apportionment of road dust

Source apportionment techniques aim to assess the pollutant mass contribution from different sources or factors to explain the variance of the pollutant concentration (Valido et al. 2018). Source apportionment analysis, which can identify the sources of pollutants, usually applies PMF which is an efficient multivariate analysis tool (Yu et al. 2016; Men et al. 2018). Although PMF requires a large number of dataset, this analysis can still be performed with n more than the number of factors involved (Banerjee et al. 2015). Previously, several studies on source apportionment of dust applied PMF analysis where the dust samples were 27–37 with more than 25 elements being analysed (Tian et al. 2018; Valido et al. 2018). The PMF model calculation is based on Eq. (4) as stated by Sulong et al. (2017) and Valido et al. (2018):

$$x_{ij} = \sum_{k=1}^p g_{ik} f_{jk} + e_{ij} \tag{4}$$

where x_{ij} is the i th concentration of element j , g_{ik} is the i th contribution of the source k , and f_{jk} is the concentration of the species j in source k , while e_{ij} are the residuals. The

values g_{ik} and f_{jk} are adjusted until the Q value was minimized as shown in Eq. (5):

$$Q = \sum_{i=1}^n \sum_{j=1}^m \left(\frac{X_{ij} - \sum_{k=1}^N g_{ik} f_{kj}}{\sigma_{ij}} \right)^2 \tag{5}$$

where n is the number of samples, m is the number of elements while σ_{ij} is the uncertainty of elements in road dust concentration of element j in i sample. The procedure of data preparation was as followed by Sulong et al. (2017). The PMF was applied using PMF version 5.0 software developed by the United States Protection Agency (USEPA). The distribution of residuals and Q values were adjusted with the number of factors determined to be six. The bioaccessible fraction from the road dust in units of $\mu\text{g g}^{-1}$ was also analyzed using PMF where the input data contained 14 elements and underwent the same processing method as the road dust elements. Then MLR analysis was performed to apportion the chemical components of road dust based on the source factors produced by PMF. Details of the procedure are explained by Amil et al. (2016).

Health risk assessments of trace metals exposure to human health

Human health risk assessments due to the exposure to non-carcinogenic and carcinogenic elements in road dust were performed based on the Risk Assessment Guidance for Superfund (USEPA 2010b). The exposure of children and adults to non-carcinogenic and carcinogenic elements from road dust were exceeded for an average daily dose (ADD) and the pathways of dermal, ingestion, and inhalation. The ADD calculation is expressed in Eq. (6) to Eq. (8) while lifetime average daily dose (LADD) for carcinogens via inhalation were calculated as in Eq. (9) as followed Jiang et al. (2016) and Han et al. (2017):

$$ADD_{inhalation} = C \times \frac{InhR \times EF \times ED}{PEF \times BW \times AT} \tag{6}$$

$$ADD_{ingestion} = C \times \frac{IngR \times EF \times ED}{BW \times AT} \times 10^{-6} \tag{7}$$

$$ADD_{dermal} = C \times \frac{SA \times SL \times ABS \times EF \times ED}{BW \times AT} \times 10^{-6} \tag{8}$$

$$LADD = \frac{C \times EF}{AT \times PEF} \times \left(\frac{InhR_{child} \times ED_{child}}{BW_{child}} + \frac{InhR_{adult} \times ED_{adult}}{BW_{adult}} \right) \tag{9}$$

where C is the concentration of trace element in road dust and the bioaccessible fraction ($\mu\text{g g}^{-1}$), InhR is the inhalation

rate ($7.6 \text{ m}^3 \text{ day}^{-1}$ for a child and $20 \text{ m}^3 \text{ day}^{-1}$ for an adult), IngR is the ingestion rate (200 mg day^{-1} for a child and 100 mg day^{-1} for an adult), EF is the exposure frequency ($180 \text{ days year}^{-1}$), ED is the exposure duration (6 years for a child and 24 years for an adult), BW is the body weight (15 kg for a child and 70 kg for an adult), PEF is the particle emission factor ($1.36 \times 10^9 \text{ m}^3 \text{ kg}^{-1}$), SA is the exposed skin area (2800 cm^2 for a child and 5700 cm^2 for an adult), SL is the skin adherence factor ($0.2 \text{ mg cm}^{-2} \text{ day}^{-1}$ for a child and $0.7 \text{ mg cm}^{-2} \text{ day}^{-1}$ for an adult), ABS is the dermal absorption factor (0.001), AT is the averaging time; non-carcinogenic = $\text{ED} \times 365 \text{ days}$; for carcinogenic = $70 \times 365 \text{ days}$). The Cr concentration was calculated as Cr (VI) which was one seventh of the total Cr concentration (Othman et al. 2019). All trace metal concentrations were calculated for the 95% upper confidence limit (UCL) to yield the estimation of the reasonable maximum exposure for non-carcinogenic and carcinogenic elements (Lu et al. 2018).

The hazard quotient (HQ) was then determined for each pathway by dividing ADD with the corresponding reference dose (RFD) while the hazard index (HI) was the sum of HQ. For the bioaccessible fraction, health risk assessments were performed for the ingestion pathway where HQ was calculated by ADD multiplied by relative bioavailability (RBA) and divided by the RFD value. RBA is the ratio of trace metal concentrations extracted using the SBET method to their total concentration in road dust. Value of HQ and HI of > 1 indicates that there is a probable risk from non-carcinogenic elements. The cancer risk (CR) determined by multiplying the ADD with corresponding slope factor (SF) while CR for the bioaccessible fraction was calculated by ADD multiply with RBA and SF. The acceptable or tolerable values are in the range $1.0\text{E}-06$ – $1.0\text{E}-04$ (Lu et al. 2018; Men et al. 2018). All the reference values were assessed via Regional Screening Level (USEPA 2010a).

Statistical analysis

The descriptive statistics and one-way ANOVA tests of trace metal, bioaccessible fraction, and ion concentrations in road dust were performed using IBM SPSS Statistic 22. Pearson correlations were also performed to identify the relationship between trace metal and ion concentrations.

Results and discussion

Chemical properties of road dust

The chemical composition of metals and ions in road dust in different urban areas in Kuala Lumpur are shown in Table 1. The highest metal concentrations were recorded for Fe for all urban areas with an average concentration of

$12169 \pm 6507 \text{ } \mu\text{g g}^{-1}$ (1.21%) with the highest concentration recorded at LRT ($23236 \pm 10141 \text{ } \mu\text{g g}^{-1}$). Al had the second highest concentrations with an average concentration of $4830 \pm 1270 \text{ } \mu\text{g g}^{-1}$ (0.48%). The sequence of Al concentrations based on the different urban areas was $\text{RD} > \text{GR} > \text{HT} > \text{CM} > \text{LRT}$. Other dominant trace metals were Zn and Mn with the highest Zn concentration recorded at LRT ($615 \pm 42.8 \text{ } \mu\text{g g}^{-1}$) and at RD ($267 \pm 158 \text{ } \mu\text{g g}^{-1}$) for Mn. Among the ion concentrations in road dust, Ca^{2+} was found to be the largest component with an average concentration of $3470 \pm 1693 \text{ } \mu\text{g g}^{-1}$ which was about 72% of the total ion concentration in road dust. Moreover, other major ions recorded were SO_4^{2-} , Na^+ , and NO_3^- with average concentrations of $560 \pm 284 \text{ } \mu\text{g g}^{-1}$, $122 \pm 69.8 \text{ } \mu\text{g g}^{-1}$, and $101 \pm 96.7 \text{ } \mu\text{g g}^{-1}$, respectively. The LRT urban area had the highest abundances for almost all metals and ions in this study while the GR urban area recorded the lowest concentrations. The sum of all trace metals represented 1.3% to 1.7% of the road dust mass and the sum of the ions represented 0.3% to 0.5% of the road dust mass. The one-way analysis of variance (ANOVA) test showed that Cl^- had significantly different ($p < 0.05$) concentrations between the different urban sites.

The spatial distribution of trace metals showed particularly high concentrations in the city center of Kuala Lumpur for Fe, Cd, Cr, Co, Cu, and Ni (Fig. 1a, b) and also Na^+ and Ca^{2+} (Fig. 1c). High anthropogenic activity in the city center was suggested to be the cause of the accumulation of these metals and ions. According to Aminiyan et al. (2017) and Men et al. (2018), high intensity human activity in one area influenced the heavy metal concentrations in the surrounding areas. The distributions of V, U, Mn, Zn, K^+ , and F^- were concentrated in the southern part of Kuala Lumpur which reflects the contribution from motor vehicles, oil burning, and combustion as high traffic numbers were observed during peak hours in the southern area. The concentrations of SO_4^{2-} accumulated in the northern, central, and southern parts also indicate the contribution of vehicle emissions in those areas. The contribution of vehicle emissions in those areas occurred due to a high number of vehicles travelling to the city center of Kuala Lumpur from northern and southern highways. Besides, there is no large industrial area in Kuala Lumpur which eliminates the industrial source for SO_4^{2-} . The scenario of people using private transportation every day to travel to the city center from the outskirts of Kuala Lumpur significantly affected the metal concentrations near the road. A hotspot was observed for Pb at the northern site and another for Cd at the central site which were the HT and CM urban sites, respectively.

The highest concentrations of Fe and Al reflect the crustal influence on road dust while the Zn and Mn concentrations suggest the influence of motor vehicles due to the Zn

Table 1 Selected trace metals and ion concentration ($\mu\text{g g}^{-1}$) in five urban areas

Element	CM $n=9$	HT $n=14$	GR $n=3$	LRT $n=5$	RD $n=5$	Overall average
Al	3816 ± 1541	5136 ± 27.1	5896 ± 1460	3214 ± 1906	6088 ± 3288	4830 ± 1270
Fe	9741 ± 3279	11024 ± 4757	6805 ± 2052	23236 ± 10,141	10041 ± 4434	12169 ± 6507
Pb	57.7 ± 29.6	89.2 ± 63.8	35.5 ± 2.66	240 ± 88.1	71.4 ± 64.4	98.8 ± 81.4
Zn	270 ± 171	365 ± 295	119 ± 20.0	615 ± 42.8	201 ± 121	314 ± 190
As	66.7 ± 39.3	106 ± 81.7	26.8 ± 11.3	70.0 ± 62.5	74.2 ± 55.2	68.8 ± 18.2
Cd	1.01 ± 0.47	0.81 ± 0.14	0.25 ± 0.17	1.00 ± 0.50	0.49 ± 0.30	0.71 ± 0.33
Cr	68.4 ± 2.14	78.6 ± 25.5	64.1 ± 4.93	90.1 ± 25.6	69.3 ± 7.11	74.1 ± 10.4
Co	4.47 ± 1.43	2.87 ± 1.42	1.04 ± 0.17	5.05 ± 2.31	3.36 ± 2.71	3.36 ± 1.00
Cu	101 ± 87.8	96.8 ± 71.5	44.1 ± 15.5	142 ± 110	50.1 ± 18.9	87.0 ± 40.5
Mn	249 ± 37.5	275 ± 116	121 ± 36.6	249 ± 140	267 ± 158	232 ± 63.0
Ni	10.2 ± 2.37	12.0 ± 7.31	5.34 ± 0.29	17.5 ± 8.08	11.5 ± 6.47	11.3 ± 3.22
U	30.0 ± 9.17	27.3 ± 19.7	7.93 ± 0.78	13.2 ± 7.24	17.2 ± 5.12	19.1 ± 9.35
V	18.2 ± 0.79	20.4 ± 6.66	20.3 ± 5.23	15.1 ± 4.67	23.1 ± 7.30	19.4 ± 2.97
Sr	15.3 ± 3.75	23.2 ± 5.94	26.9 ± 12.0	24.0 ± 4.60	21.0 ± 2.82	22.1 ± 3.94
Na ⁺	128 ± 18.4	115 ± 58.9	74.7 ± 43.5	154 ± 106	124 ± 98.7	122 ± 69.8
NH ₄ ⁺	103 ± 18.3	83.8 ± 55.8	84.2 ± 82.7	88.4 ± 40.9	135 ± 97.2	96.5 ± 61.9
K ⁺	371 ± 79.3	315 ± 103	170 ± 79.2	392 ± 255	313 ± 99.3	327 ± 305
Ca ²⁺	3879 ± 753	3380 ± 1432	2363 ± 972	4394 ± 2144	2729 ± 215	3470 ± 1693
F ⁻	14.4 ± 1.11	11.6 ± 5.42	9.19 ± 3.88	18.1 ± 12.0	12.0 ± 9.55	13.1 ± 6.90
Cl ⁻	34.5 ± 3.71	49.7 ± 26.3	52.3 ± 39.7	72.7 ± 14.8	38.4 ± 12.2	47.7 ± 23.8
Br ⁻	60.4 ± 10.4	56.6 ± 16.0	32.3 ± 16.5	64.3 ± 24.7	41.4 ± 7.86	54.5 ± 22.3
NO ₃ ⁻	59.2 ± 17.6	98.7 ± 16.0	94.4 ± 19.9	196 ± 87.3	94.8 ± 31.1	101 ± 96.7
SO ₄ ²⁻	607 ± 79.3	572 ± 255	442 ± 133	565 ± 387	508 ± 150	560 ± 284

contained in lubricant oil, tyres, and carburetors (Arslan 2001; Al-Khashman 2004; Jayarathne et al. 2017). Moreover, high concentrations of SO₄²⁻ and NO₃⁻ indicate the contribution of motor vehicle emissions as they originate from SO₂ and NO₂ (Morawska et al. 2008) while is Ca²⁺ suggested to be influenced by the crustal source where calcium usually occurred in the soil constituent and is often applied as a filler in road surface material (Limbeck et al. 2009). Our result supports this with the highest SO₄²⁻ concentrations at CM while NO₃⁻ was recorded highest at the LRT urban area where both locations have high exposures to motor vehicle emissions as well as emissions from rail transportation. Pearson correlation test results showed that there were significant correlations ($p < 0.01$) between metals such as Cd, Cr, Cu, Mn, Ni, V which suggests the same source for these elements (Table S3).

Trace metal and selected ion (SO₄²⁻ and NO₃⁻) concentrations were compared with other cities (Table S4). Higher trace metal concentrations were recorded by Han et al. (2013) in Kuala Lumpur compared to the overall average trace metal concentrations in this study. However, Fe, Pb, and Zn in the LRT urban area had higher concentrations where contributions from rail transportation may be the cause. Higher metal concentrations were recorded by Padoan et al.

(2017) who studied roadside metals in Turin, Italy, when compared to this study except for Pb and Zn. High metal concentrations were reported to be sourced from traffic, various human activities, and gasoline fuel additives. Higher Fe, Mn, and Ni concentrations were recorded by Men et al. (2018) compared to this study in Beijing city, where Cd had concentrations recorded at eight times higher than the background concentration. A study by Shi and Lu et al. (2018) found higher concentrations for certain metals such as Cr, Co, Ni, and V. Ramírez et al. (2018) studied metal and ion concentrations in the thoracic fraction of road dust in Bogota city found higher concentrations of Al, Fe, NO₃⁻, and SO₄²⁻ than this study and suggested that road dust was the main source of PM₁₀ concentrations. The concentration of trace metals was compared with soil samples in Kuala Lumpur where Othman et al. (2019) recorded concentrations of Mn that were about 1.3 times higher than this study while other trace metals recorded lower concentrations. As for comparison, the concentration of Pb and Ar in garden soil in Johannesburg recorded by Mathee et al. (2018) where lower concentrations were reported compared to this study with suggestion that metals in soil also effected the health of school children in high traffic city area where high concentration of metals was observed in blood sample.

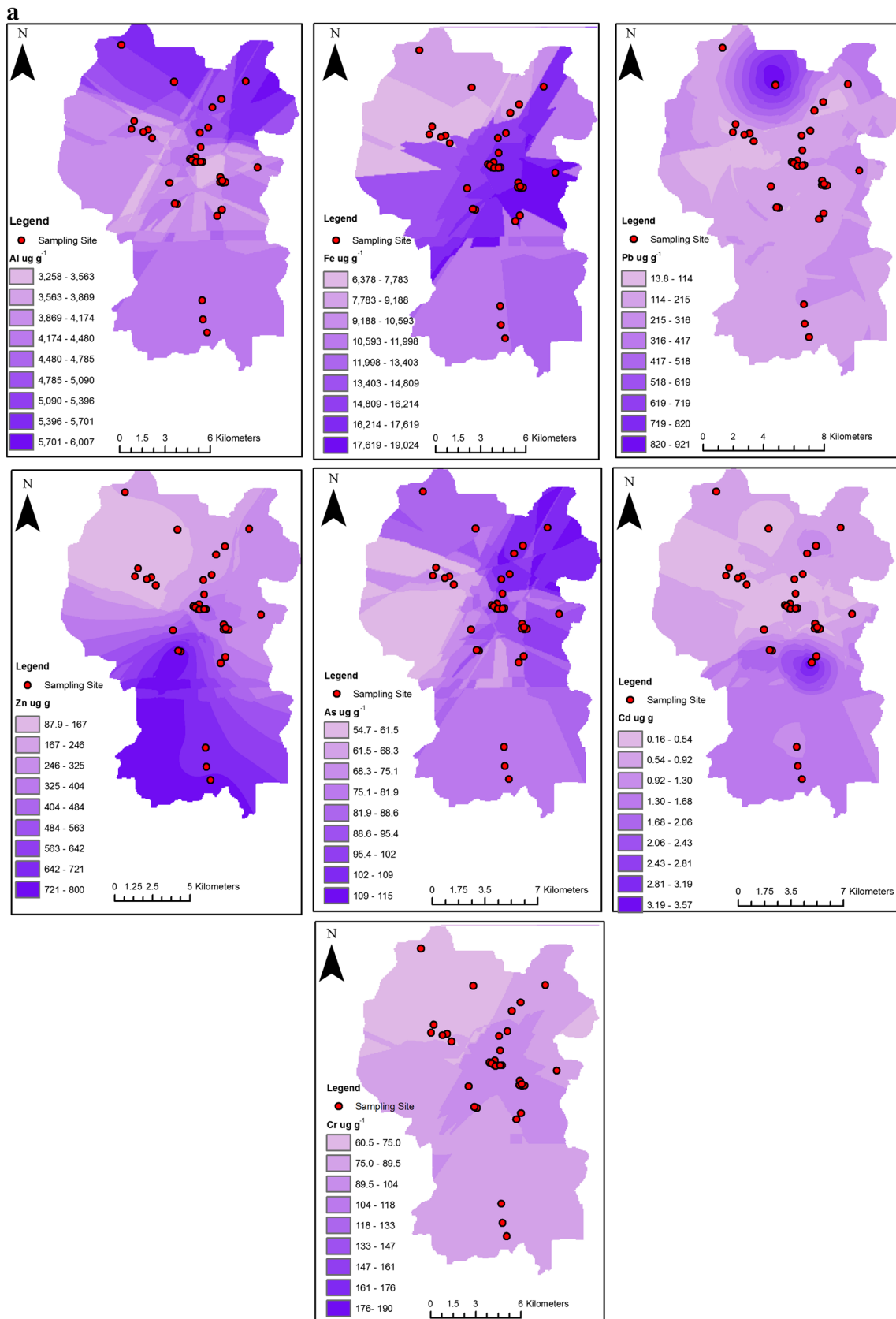


Fig. 1 **a** Spatial distribution of Al, Fe, Pb, Zn, As, Cd, and Cr concentration in road dust in Kuala Lumpur. **b** Spatial distribution of Co, Cu, Mn, Ni, U, V, and Sr concentration in road dust in Kuala Lumpur. **c** Spatial distribution of ion concentration in road dust in Kuala Lumpur

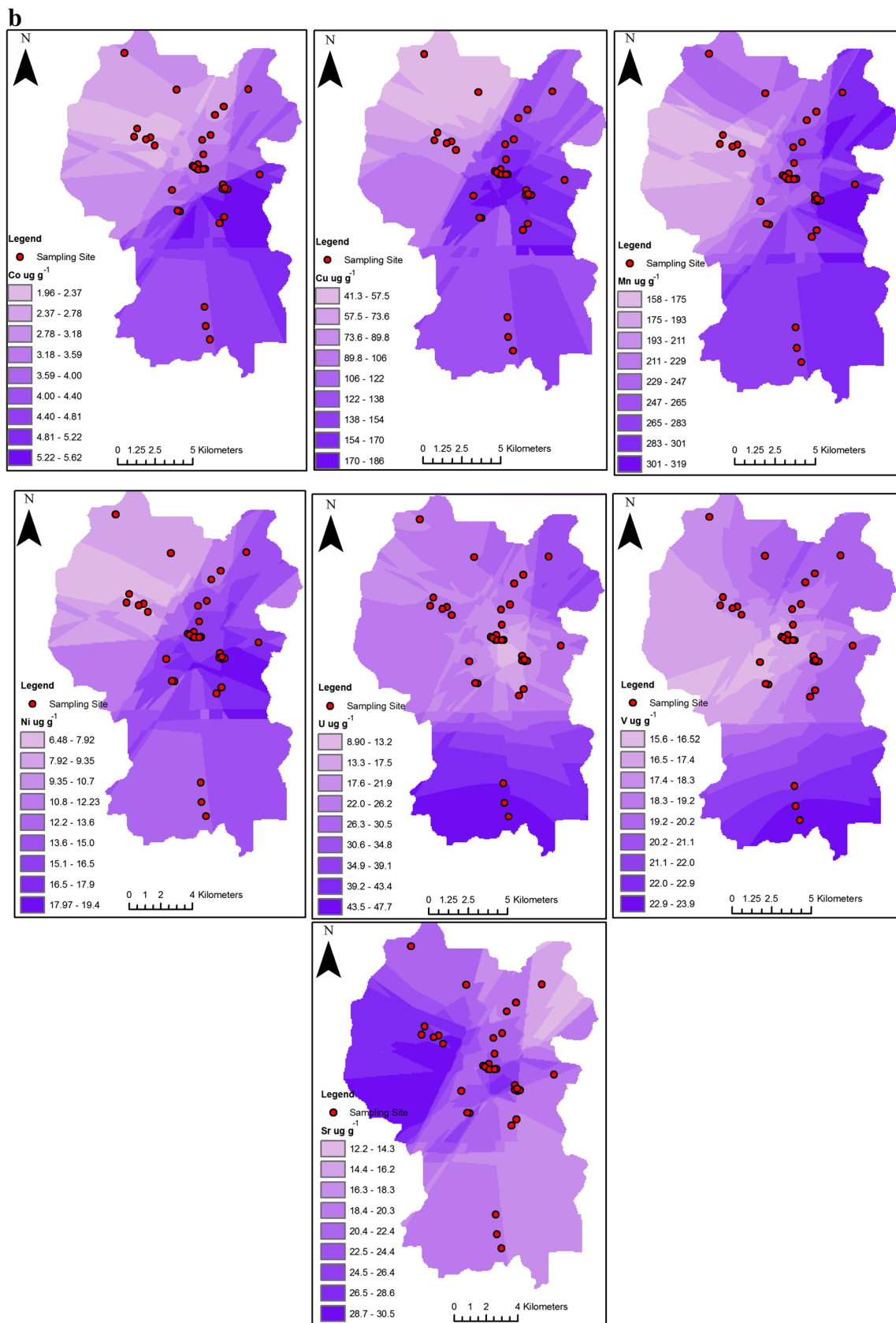


Fig. 1 (continued)

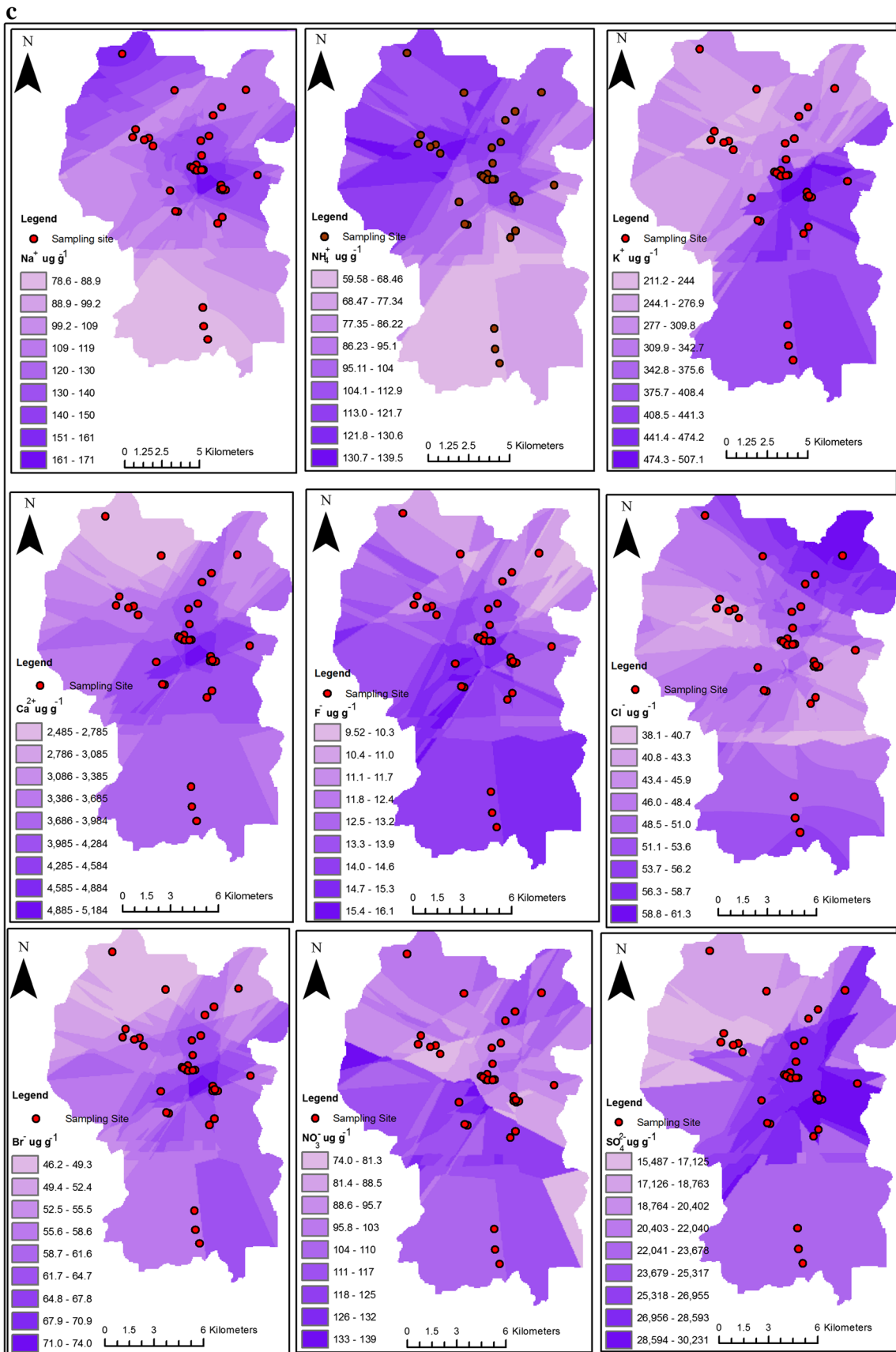


Fig. 1 (continued)

Bioaccessible fraction of road dust

The results for all analyzed elements of the bioaccessible fraction and comparisons with other cities are listed in Table 2. Overall, the highest bioaccessibility was recorded for Zn with an average of 28.6% followed by Sr with overall average of 20.5%. The concentrations bioaccessible Zn were highest at LRT while for Sr, was highest were at RD. Cd and Cr both recorded bioaccessibilities of 13.4% to 24.0% while the least bioaccessible trace metals were Al and Fe; Al and Fe had overall bioaccessibility averages below 1%. The one-way ANOVA tests showed that there were significant differences ($p < 0.05$) for the U concentrations collected at different areas in Kuala Lumpur. The results of the Pearson correlations showed that there were significant correlations ($p < 0.01$) between almost all trace metal fractions and Al and Fe which suggests high contributions from the earth crust source in the bioaccessible fraction of road dust (Table S5).

Low bioaccessibility for Fe with high concentrations for Zn is consistent with a study by Padoan et al. (2017) who also had a sequence of bioaccessibility of Zn > Pb > Cu > Mn > Sb > Fe > Ni > Cr. As reported by Valido et al. (2018), bioaccessibility of metals, especially those produced naturally, is less than metals produced from high emission processes. A study by Patinha et al. (2015) found bioaccessibility in the range of 3.1–18.1% for Fe which is higher than this study. Overall, there was a significant difference ($p < 0.05$) for total metal concentration in road dust compared to bioaccessible fraction. This finding is consistent with Goix et al. (2016) that suggested bioaccessible fraction concentration is controlled by

the element of physical and chemical speciation related to its valence state, adsorption onto clay mineral, oxides, and/or its presence as constituent of mineral. Moreover, size of the particle, solid-phase properties, metal interaction, and mineralogy composition may affect the bioaccessible fraction concentration (Yu et al. 2014; Patinha et al. 2015; Drahota et al. 2017). The high bioaccessibility of Zn was also consistent with a study in urban areas of Ottawa, Canada (Rasmussen et al. 2008), Nanjing, China (Hu et al. 2011), and Kank, Republic Check (Drahota et al. 2017) while in Barcelona, Spain (Valido et al. 2018), the highest bioaccessibility was recorded for Ni. The spatial distributions of the highest bioaccessible metals (Zn, Sr, Cd, and Cr) were explored, where similar spatial patterns were observed (Figure S2). All these elements showed high bioaccessibility in the northwest region and in the central region. The high bioaccessible fraction in the northwest may originate from traffic emissions coupled with anthropogenic that is which located in this commercial urban area.

Pollution assessment of road dust

To assess the trace metal concentrations in road dust based on different urban areas, *Igeo*, PI, and EF were calculated (Figure S3). The results for *Igeo* followed the sequence of As > Cd > U > Pb > Zn > Cu > Cr > Fe > Mn > Co > Ni > V > Sr > Al. Based on the *Igeo* classification, the road dust samples were classified as uncontaminated for Al, Fe, Cr, Co, Mn, Ni, V, and Sr, moderately contaminated for Pb, Zn, Cu, and U, moderately to strongly contaminated for Cd and strongly to extremely contaminated for As. The HT and RD

Table 2 Mean percentage (%) and standard deviation (SD) of trace metals in bioaccessible fraction compared to other cities

		Al	Fe	Pb	Zn	As	Cd	Cr	Co	Cu	Mn	Ni	U	V	Sr
CM (n = 9)	Mean	0.42	0.55	1.02	33.6	0.97	21.8	16.9	7.40	18.8	5.37	7.33	0.11	1.39	22.1
	SD	0.30	0.48	0.69	26.0	0.45	9.87	1.46	7.14	29.2	3.59	4.52	0.10	0.80	13.0
HT (n = 14)	Mean	0.99	0.60	1.28	25.7	1.16	13.4	15.2	6.32	9.67	7.14	7.65	0.18	1.39	15.8
	SD	0.66	0.28	1.58	21.5	1.08	5.52	4.83	5.83	4.53	8.74	8.94	0.06	0.93	13.1
GR (n = 3)	Mean	0.21	0.56	1.42	15.3	2.33	24.0	17.4	8.57	8.75	9.34	6.23	0.67	0.85	18.7
	SD	0.08	0.25	0.67	4.00	0.36	19.3	0.61	3.91	2.57	6.46	0.90	0.44	0.09	9.02
LRT (n = 5)	Mean	0.99	1.29	1.25	37.2	2.79	16.8	14.5	10.84	9.10	8.76	17.9	0.71	2.02	22.1
	SD	0.85	0.71	1.02	34.5	1.29	11.3	3.66	9.20	1.11	3.96	7.75	0.70	1.35	16.0
RD (n = 5)	Mean	0.41	0.43	1.08	31.2	2.45	14.0	16.8	5.44	12.7	4.95	8.74	0.21	0.97	23.8
	SD	0.22	0.24	1.12	15.6	1.71	7.09	2.47	2.82	5.58	4.29	6.94	0.19	0.74	20.1
Overall	Mean	0.50	0.69	1.21	28.6	1.94	18.0	16.1	7.72	11.8	7.11	9.59	0.38	1.32	20.5
	SD	0.42	0.39	0.78	20.3	0.98	10.6	2.61	5.78	8.61	5.41	5.81	0.30	0.78	14.2
Ottawa (Rasmussen et al. 2008)					65					44		44			
Nanjing (Hu et al. 2011)			3.88	47	60.1	38.8	74.5	5.83	22.1	29.8	47.6	15.7		11.2	
Kank (Drahota et al. 2017)				27.4	65.6	7.5				26.6					
Turin (Padoan et al. 2017)				27.8	51.5					21.2		1.9			
Barcelona (Valido et al. 2018)		1	1	27	16		30	20	21	36	24	44	4		28

areas had As values of 5.5 and 5, respectively, which indicated that both urban areas are extremely polluted with As. The lowest *Igeo* value was recorded for Al at LRT with a value of -5.2 followed by Sr at CM with a value of -5.1 . A study by Li et al. (2017) found the highest mean value of Cd in street dust located in a commercial area. The highest *Igeo* value recorded by As was also consistent with the results for PI and EF where As had the highest values, indicating high levels of pollution and extreme contributions from anthropogenic sources. The highest PI value for As was recorded at HT (66.4) while high EF values were recorded at HT and LRT. The EF value for GR was relatively low compared to other urban areas for almost all trace metals while LRT recorded the highest EF values for all trace metals suggesting high pollution loads in the road dust for this area. As reported by Li et al. (2017), socioeconomic activities and other factors such as high temperatures which accelerate corrosion of metals causing the release of metals in the environment are causes. A study by Shi and Lu et al. (2018) had Pb values in the range 5–20 which indicated that trace metals have accumulated at different levels in road dust with particle sizes smaller than $63\ \mu\text{m}$; there was significant enrichment particularly in Xi'an, China. The possible sources of the enrichment of Pb in road dust are fossil fuel combustion, metal processing, wear and tear of tyre, road paint, brake lining, and corrosion of galvanized of the road divider (Cao et al. 2011; Rastmanesh et al. 2017).

Source apportionment of road dust and the bioaccessible fraction

The sources of trace metals and ions in road dust and trace metals in the bioaccessible fraction were identified using the PMF method. Overall, six factors were identified for both road dust and the bioaccessible fraction as presented in Fig. 2. The relative contributions of the sources are shown in Figure S4.

Road dust

Factor 1 is represented by high factor loadings of NH_4^+ (56%), Br^- (40%), Ca^{2+} (37%), Na^+ (33%), and these elements are closely related to the earth's crust. This factor represents a 2% contribution to the road dust contamination sources. According to Xie et al. (2009), NH_4^+ originates from ammonia from fertilizer manufacturing plants and agricultural activities while Al-Khashman (2007) and Kong et al. (2011) also reported high CaCO_3 in street dust which was suggested to be sourced from the earth's crust. A further source of Ca was also suggested to be construction activity which uses cement as a building materials (Liu et al. 2017).

Factor 2 is characterized by the elements SO_4^{2-} (49%), Zn (26%), F^- (25%), and Cu (24%), identified as from vehicle emissions. The contribution of this factor was 2% of the total

road dust contamination sources. Some studies have suggested that SO_4^{2-} is derived from gas-to-particle conversion processes (Behera and Sharma 2012; Liu et al. 2017). Zn has also been classified as be related to traffic and vehicular activities, particularly from tyre wear and Zn use in tyre production (Kong et al. 2011; Men et al. 2018).

Factor 3 is identified by the elements of U (81%), As (72%), Cd (45%), and Mn (35%). This factor is identified as industrial activity and represents a 3% contribution to road dust contamination sources. U has been observed to be a dominant contribution to pollution at phosphoric acid production plants and also associated with coal and fly ash (McCartney et al. 2000; Cayir et al. 2012). Moreover, As, Cd, and Mn are considered the main elements indicating industrial activities and coal combustion (Rahman et al. 2011; Bhuiyan et al. 2015; Liang et al. 2017). Industrial emissions and combustion produce fly ash that can be deposited as road dust (Men et al. 2018).

Factor 4 includes Cu (57%), Sr (55%), Zn (54%), and Ni (43%). Cu and Zn were suggested to be from metal parts of cars, brake wear, and additives in lubrication oil in two-stroke engines (Liu et al. 2017; Valido et al. 2018). This factor was identified as vehicle and traffic activity which represent a 47% contribution to road dust pollution sources.

The elements K^+ (75%), Na^+ (44%), F^- (37%), and SO_4^{2-} (32%) represent factor 5 which is the soil element and fossil fuel source factor, contributing 39% to the road dust contamination source. The element K^+ occurred due to soil-associated element where larger particle is likely to be associated with road dust resuspension (Gietl et al. 2010). Meanwhile, F^- and SO_4^{2-} originated from engine fuel combustion which produces SO_2 . This was then transformed to SO_4^{2-} (Zhao et al. 2006; Othman et al. 2019).

Next, factor 6 is represented by NO_3^- (79%), Al (42%), V (40%), and Cl^- (33%). It is identified as an oil combustion factor with 7% contribution to road dust contamination. It contains high loadings of NO_3^- which are closely related to vehicle exhaust. This factor is related to NO_3^- as it underwent gas-to-particle conversion process and NO_3^- was produced during the combustion (Liu et al. 2017). Sulong et al. (2017) also had a similar finding, in which NO_3^- was found from a high volume of traffic, i.e., exhaust emissions in Kuala Lumpur.

Bioaccessible fraction

According to the PMF results, factor 1 was represented by the elements Fe (80%), Co (56%), Zn (45%), and Sr (36%). Factor 1 was identified as soil dust due to the particularly high factor load of Fe. Fe usually has abundance concentrations in soil and the earth's crust which are the dominant compositions of road dust (Padoan et al. 2017). The contribution of this factor was 50% of the bioaccessible fraction pollution source.

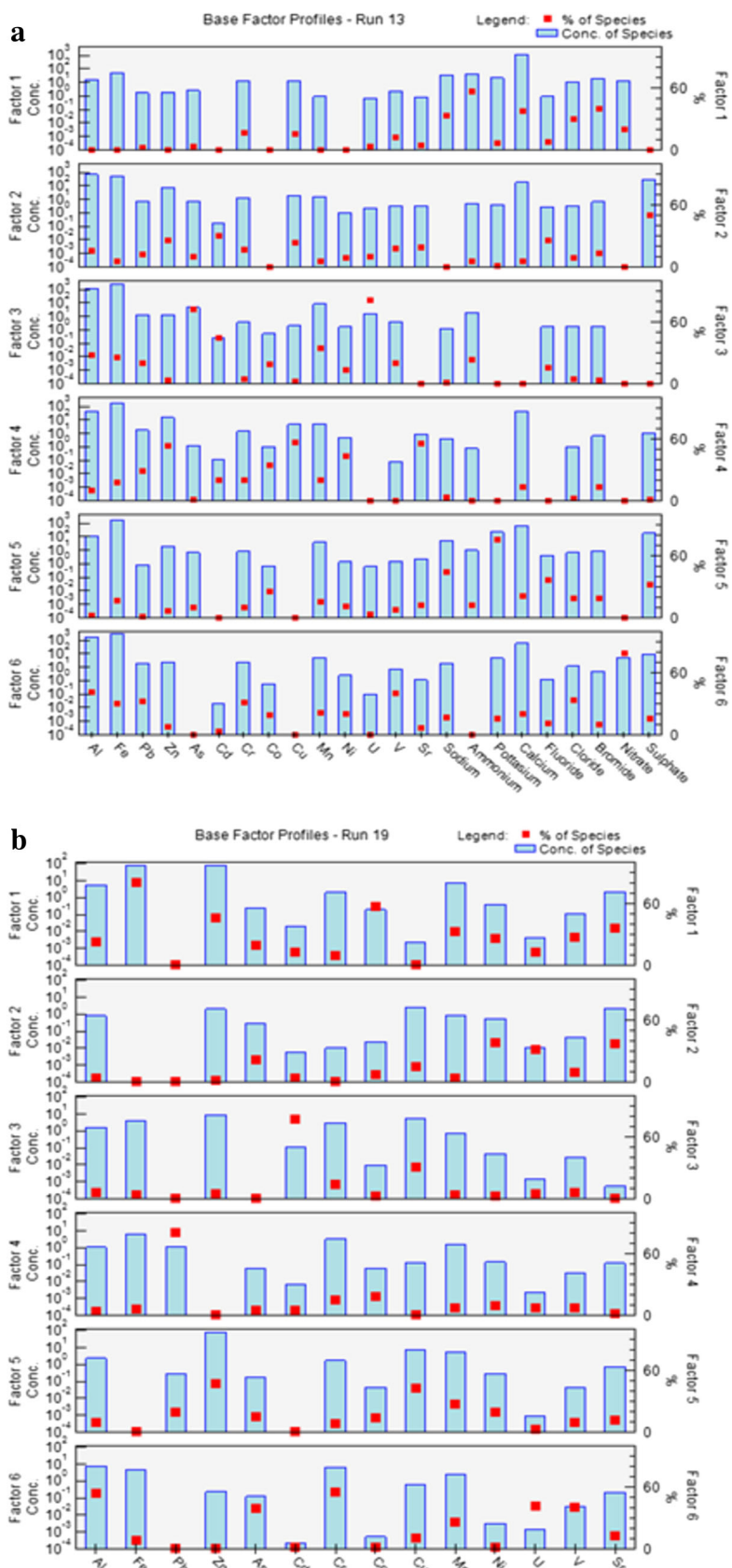


Fig. 2 PMF result for **a** trace metals and water soluble ions in road dust and **b** trace metals in bioaccessible fraction

Factor 2 was characterized as industrial activity with contributions of Ni (38%), Sr (37%), U (31%), and As (21%). This factor was identified as from manufacturing activities—as reported by Kabadayi and Cesur (2010), Ni is used in electroplating, electroforming, and nickel-cadmium batteries. Al-Khashman (2004) also reported Ni application in the production of office furniture and as an additive layer to vehicle bodywork. Other elements such as Sr, U, and As are also suggested to be contributed from manufacturing industries. The factor represents as 2% of the bioaccessible fraction pollution sources.

Industrial activity was identified for factor 3 with contributions of Cd (77%), Cu (30%), V (6.29%), and Al (6.25%) and making up 4% of the bioaccessible fraction source. As reported by Charlesworth et al. (2003) and Shi et al. (2008), Cd is usually associated with industrial activities where, according to Kabadayi and Cesur (2010), Cd was proved to have high concentrations in industrial areas. V is associated with electric utility company's combustion of oil in large industrial and commercial sources (Qing et al. 2007; Othman et al. 2019).

Factor 4 was mainly sourced from road paint with the highest contribution from Pb (80%). Other contributors were Cr (14%), Ni (9.9%), and V (7.01%), making up 3% of the total bioaccessible fraction pollution source. Pb has the highest factor loading; thus, only this element is considered as the contributing element. Pb particles were originated from paint applied on the road surface (Al-Khashman 2007; Chen et al. 2014).

Factor 5 included about 47%, 42%, 26%, and 19% of the concentrations of Zn, Cu, Mn, and Ni. Zn and Cu were suggested to originate from traffic and motor vehicles (Shi et al. 2008; Jayarathne et al. 2017) with a contribution of 34% to the bioaccessible fraction pollution sources. Referring to Jiries (2001) and Al-Khashman (2004), Zn and Cu can be produced from mechanical abrasion where these elements were used in brake lining and other vehicle parts. Moreover, Mn was also suggested to be from an anthropogenic source including Mn ore exploitation, alloy production, and gasoline additive (Rodrigues et al. 2018).

Factor 6 accounted for 53% to 39% of the concentrations of Al, U, V, and As. All these elements are closely related to natural and coal combustion and represented 7% of the bioaccessible fraction pollution sources. Al, which was highly abundant, was suggested to have a natural source while U and V were suggested to originate from coal combustion (Cayir et al. 2012; Othman et al. 2019).

Health risk assessment of road dust and the bioaccessible fraction

The exposure risk posed by non-carcinogenic and carcinogenic elements was modeled using the human health risk assessment (Ali et al. 2017). The health risk assessment for a child

and an adult for inhalation, ingestion, and dermal pathways at each urban area are listed in Table 3, Table 4, and Table 5. The HQ values of all studied metals for both children and adults were below the safe value ($HQ < 1$) for all pathways. However, total HQ (HI) for HT and LRT both recorded values of > 1 for a child for the ingestion pathway. For the ingestion and dermal pathways, the highest HI was 2.0E+00 (child) and 1.9E-02 (adult), respectively, both recorded for LRT. The sequence of urban areas based on HI values for inhalation and dermal was LRT > HT > RD > CM > GR and for ingestion was LRT > HT > COM > RD > GR.

The CR value for the inhalation pathway was calculated by taking into account both child and adult as only one CR value. The highest total CR value was recorded for the LRT urban area with a value of 3.3E-08 while the lowest total CR value was recorded for GR with a value of 6.4E-09. For the ingestion pathway, all carcinogenic elements had values within the range 1.0E-06–1.0E-04 except for As that exceeded 1.0E-04 at HT, LRT, and RD, indicating a probable risk from this carcinogenic element. For the dermal pathway, all carcinogenic elements recorded values in range 8.9E-09–1.9E-05 where As recorded the highest CR value for an adult in all urban areas but this was still in the tolerable limit range. Overall, the sequence of urban areas based on total CR values for inhalation was LRT > HT > RD > CM > GR while for ingestion it was LRT > RD > HT > CM > GR and for dermal it was GR > LRT > RD > HT > CM. The risk to a child for carcinogenic effects was 0.2 to 1.2 times higher compared to an adult for the ingestion pathway while the risk for an adult was 1.45 to 1.6 times (non-carcinogenic) and 5.8 to 6.3 times (carcinogenic) higher compared to a child for the dermal pathway.

Overall, the sequence of exposure pathways was ingestion > dermal > inhalation which is consistent with studies by Shi et al. (2011), Ali et al. (2017), Li et al. (2018), and Men et al. (2018). The highest As values for HQ and CR in this study were suggested to reflect high As concentrations in road dust for locations with high traffic volumes such as LRT and HT. High As concentrations were suggested to originate from anthropogenic activities especially in urban area where, according Othman et al. (2019), the As concentration in Kuala Lumpur soil was 10.8 $\mu\text{g g}^{-1}$. As reported by Amjadian et al. (2018), higher carcinogenic values reflected their background levels in the studied locations more than the anthropogenic sources. Child exposure compared to adult was suggested to be 8.2 times higher for the ingestion pathway while inhalation and dermal was two times higher (Shi et al. 2011). A study by Kurt-Karakus (2012) and Ali et al. (2017) both found higher HQ valued for an adult for indoor dust and road dust, respectively, compared to a child via the dermal pathway which consistent with this study. A higher adult risk for dermal pathway was due to higher skin exposure of an adult compared to a child. However, due to the habits of children

Table 3 Hazard quotient (HQ) for child and adult and cancer risk (CR) for both child and adult exposure via inhalation pathway

	GR		CM		HT		LRT		RD	
	Child HQ	Adult HQ	Child HQ	Adult HQ	Child HQ	Adult HQ	Child HQ	Adult HQ	Child HQ	Adult HQ
Min	1.6E-06	9.2E-07	2.6E-06	1.5E-06	2.6E-06	1.5E-06	3.2E-06	1.8E-06	3.6E-06	2.0E-06
Cu	3.8E-07	2.1E-07	7.8E-07	4.4E-07	6.4E-07	3.6E-07	1.3E-06	7.2E-07	3.4E-07	1.9E-07
Zn	1.0E-07	5.9E-08	2.5E-07	1.4E-07	3.3E-07	1.9E-07	7.1E-07	4.0E-07	2.2E-07	1.2E-07
Ni	1.0E-07	5.7E-08	2.6E-07	1.5E-07	2.7E-07	1.5E-07	4.6E-07	2.6E-07	3.3E-07	1.8E-07
Cr (VI)	6.7E-07	3.8E-07	6.4E-07	3.6E-07	8.2E-07	4.6E-07	1.1E-06	6.0E-07	6.8E-07	3.9E-07
Cd	7.2E-08	4.0E-08	3.8E-07	2.2E-07	2.0E-07	1.2E-07	4.4E-07	2.5E-07	1.6E-07	9.0E-08
Al	1.8E-06	9.9E-07	9.2E-07	5.2E-07	1.2E-06	7.0E-07	1.0E-06	5.8E-07	1.9E-06	1.1E-06
Pb			1.1E-09		2.1E-09		3.3E-09		1.9E-08	3.9E-09
As	3.4E-05	1.9E-05	5.9E-05	3.3E-05	9.5E-05	5.4E-05	9.0E-05	5.1E-05	8.7E-05	4.9E-05
Fe	3.1E-06	1.8E-06	3.2E-06	1.8E-06	3.6E-06	2.1E-06	1.8E-05	1.0E-05	4.1E-06	2.3E-06
Co	8.9E-07	5.0E-07	4.8E-06	2.7E-06	2.3E-06	1.3E-06	4.8E-06	2.7E-06	4.1E-06	2.3E-06
U	6.0E-07	3.4E-07	3.1E-06	1.8E-06	2.4E-06	1.4E-06	2.0E-06	1.2E-06	2.0E-06	1.1E-06
V	1.2E-06	6.9E-07	7.4E-07	4.1E-07	9.0E-07	5.1E-07	7.7E-07	4.3E-07	1.2E-06	6.7E-07
Sr	3.5E-07	2.0E-07	7.3E-08	4.1E-08	1.1E-07	6.3E-08	9.3E-11	5.1E-08	1.5E-07	8.5E-08
Total	4.5E-05	2.5E-05	7.7E-05	4.3E-05	1.1E-04	6.3E-05	1.7E-08	7.0E-05	1.1E-04	6.0E-05

Table 4 Hazard quotient (HQ) and cancer risk (CR) for child and adult exposure via ingestion pathway

GR	COM						HT						LRT						RD					
	Adult		Child		Adult		Child		Adult		Child		Adult		Child		Adult		Child		Adult			
	HQ	CR	HQ	CR	HQ	CR	HQ	CR	HQ	CR	HQ	CR	HQ	CR	HQ	CR	HQ	CR	HQ	CR	HQ	CR		
Min	5.8E-02	1.2E-02	9.2E-02	2.0E-02	9.5E-02	2.0E-02	2.0E-02	2.0E-02	2.0E-02	2.0E-02	1.2E-01	2.5E-02	2.5E-02	1.3E-01	9.1E-04									
Cu	1.4E-02	2.9E-03	2.8E-02	6.0E-03	2.3E-02	6.0E-03	4.9E-03	4.9E-03	4.9E-03	4.9E-03	4.6E-02	9.8E-03	9.8E-03	1.2E-02	8.6E-05									
Zn	3.7E-03	8.0E-04	8.8E-03	1.9E-03	1.2E-02	1.9E-03	2.6E-03	2.6E-03	2.6E-03	2.6E-03	2.6E-02	5.5E-03	5.5E-03	7.7E-03	5.5E-05									
Ni	3.6E-03	5.8E-06	9.4E-03	1.5E-05	9.8E-03	1.3E-05	1.6E-05	1.6E-05	1.6E-05	1.6E-05	1.4E-05	2.6E-05	2.6E-05	1.2E-02	8.4E-05	1.6E-05								
Cr (VI)	2.4E-02	3.1E-06	2.3E-02	3.0E-06	2.9E-02	3.8E-06	3.8E-06	3.8E-06	3.8E-06	3.8E-06	3.2E-06	4.9E-06	4.9E-06	2.4E-02	1.7E-04	2.7E-06								
Cd	2.6E-03	5.5E-04	1.4E-02	2.9E-03	7.3E-03	2.9E-03	1.6E-03	1.6E-03	1.6E-03	1.6E-02	3.4E-03	3.4E-03	3.4E-03	5.7E-03	4.1E-05									
Al	6.3E-02	1.3E-02	3.3E-02	7.0E-03	4.5E-02	7.0E-03	9.5E-03	9.5E-03	9.5E-03	3.7E-02	7.9E-03	7.9E-03	7.9E-03	6.7E-02	4.8E-04									
Pb	1.2E-05	1.0E-05	2.3E-05	2.3E-05	1.9E-05	3.6E-05	3.6E-05	3.6E-05	3.6E-05	3.1E-05	2.0E-04	2.0E-04	2.0E-04	4.3E-05	3.7E-05									
As	3.6E-01	4.7E-05	2.9E-01	8.2E-05	7.0E-05	4.6E-01	1.3E-04	1.3E-04	1.3E-04	1.1E-04	8.2E-01	6.9E-01	6.9E-01	1.2E-04	2.2E-02	1.0E-04								
Fe	1.1E-01	2.4E-02	1.2E-01	2.5E-02	1.3E-01	2.8E-02	2.8E-02	2.8E-02	2.8E-02	6.4E-01	1.4E-01	1.4E-01	1.4E-01	1.5E-01	1.0E-03									
Co	3.2E-02	6.8E-03	1.7E-01	3.6E-02	8.2E-02	3.6E-02	1.8E-02	1.8E-02	1.8E-02	1.7E-01	3.7E-02	3.7E-02	3.7E-02	1.5E-01	1.1E-03									
U	2.2E-02	4.6E-03	1.1E-01	2.4E-02	8.6E-02	2.4E-02	1.8E-02	1.8E-02	1.8E-02	7.3E-02	1.6E-02	1.6E-02	1.6E-02	7.1E-02	5.1E-04									
V	4.4E-02	9.4E-03	2.6E-02	5.6E-03	3.2E-02	5.6E-03	6.9E-03	6.9E-03	6.9E-03	2.8E-02	5.9E-03	5.9E-03	5.9E-03	4.2E-02	3.0E-04									
Sr	1.3E-02	3.2E-05	2.6E-03	6.8E-06	5.8E-06	5.6E-04	1.0E-05	8.5E-04	8.5E-04	8.7E-06	3.3E-03	8.4E-06	8.4E-06	7.2E-06	3.9E-05	1.2E-05								
Total	7.5E-01	9.9E-05	9.3E-01	1.3E-04	1.4E+00	5.9E-01	2.0E-04	8.5E-01	8.5E-01	1.7E-04	2.0E+00	3.7E-04	9.5E-01	8.0E-01	2.7E-02	1.7E-04								

Table 5 Hazard quotient (HQ) and cancer risk (CR) for child and adult exposure via dermal pathway

GR	COM						HT						LRT						RD					
	Child HQ	Child CR	Adult HQ	Adult CR	Child HQ	Child CR	Adult HQ	Adult CR	Child HQ	Child CR	Adult HQ	Adult CR	Child HQ	Child CR	Adult HQ	Adult CR	Child HQ	Child CR	Adult HQ	Adult CR				
Min	1.6E-04	2.5E-04	2.6E-04	3.9E-04	2.7E-04	4.0E-04	3.3E-04	4.0E-04	3.3E-04	5.0E-04	3.6E-04	5.0E-04	3.6E-04	5.0E-04	3.6E-04	5.0E-04	3.6E-04	5.0E-04	3.6E-04	5.0E-04				
Cu	3.8E-05	5.8E-05	7.8E-05	1.2E-04	6.4E-05	9.8E-05	1.3E-04	9.8E-05	1.3E-04	2.0E-04	3.4E-05	2.0E-04	3.4E-05	2.0E-04	3.4E-05	2.0E-04	3.4E-05	2.0E-04	3.4E-05	2.0E-04				
Zn	1.0E-05	1.6E-05	2.5E-05	3.8E-05	3.3E-05	5.1E-05	7.1E-05	5.1E-05	7.1E-05	1.1E-04	2.2E-05	1.1E-04	2.2E-05	1.1E-04	2.2E-05	1.1E-04	2.2E-05	1.1E-04	2.2E-05	1.1E-04				
Ni	1.0E-05	1.6E-08	2.6E-05	4.0E-05	2.6E-07	4.2E-08	4.6E-05	4.2E-05	4.6E-05	7.4E-08	7.0E-05	4.5E-07	7.4E-08	7.0E-05	4.5E-07	7.4E-08	7.0E-05	4.5E-07	7.4E-08	7.0E-05				
Cr (VI)	6.7E-05	8.6E-09	6.4E-05	8.3E-09	5.1E-08	8.2E-05	1.1E-08	1.3E-04	6.5E-08	1.4E-08	8.4E-08	1.4E-08	8.4E-08	1.4E-08	8.4E-08	1.4E-08	8.4E-08	1.4E-08	8.4E-08	1.4E-08				
Cd	7.2E-06	1.1E-05	3.9E-05	5.9E-05	2.1E-05	3.1E-05	4.4E-05	3.1E-05	4.4E-05	6.7E-05	1.6E-05	6.7E-05	1.6E-05	6.7E-05	1.6E-05	6.7E-05	1.6E-05	6.7E-05	1.6E-05	6.7E-05				
Al	1.8E-04	2.7E-04	9.2E-05	1.4E-04	1.2E-04	1.9E-04	1.0E-04	1.9E-04	1.0E-04	1.6E-04	1.9E-04	1.6E-04	1.9E-04	1.6E-04	1.9E-04	1.6E-04	1.9E-04	1.6E-04	1.9E-04	1.6E-04				
Pb	3.3E-08	2.0E-07	6.4E-08	9.1E-07	3.9E-07	1.0E-07	6.2E-07	1.0E-07	6.2E-07	5.7E-07	3.5E-06	5.7E-07	3.5E-06	5.7E-07	3.5E-06	5.7E-07	3.5E-06	5.7E-07	3.5E-06	5.7E-07				
As	3.4E-03	1.3E-07	6.0E-03	2.3E-07	1.4E-06	9.6E-03	3.7E-07	1.5E-02	2.3E-06	9.1E-03	3.5E-07	1.4E-02	3.5E-07	1.4E-02	3.5E-07	1.4E-02	3.5E-07	1.4E-02	3.5E-07	1.4E-02				
Fe	3.1E-04	4.8E-04	3.2E-04	4.9E-04	3.7E-04	5.6E-04	1.8E-03	5.6E-04	1.8E-03	2.7E-03	4.1E-04	2.7E-03	4.1E-04	2.7E-03	4.1E-04	2.7E-03	4.1E-04	2.7E-03	4.1E-04	2.7E-03				
Co	8.9E-05	1.4E-04	4.8E-04	7.3E-04	2.3E-04	3.5E-04	4.9E-04	3.5E-04	4.9E-04	7.4E-04	4.1E-04	7.4E-04	4.1E-04	7.4E-04	4.1E-04	7.4E-04	4.1E-04	7.4E-04	4.1E-04	7.4E-04				
U	6.1E-05	9.2E-05	3.1E-04	4.8E-04	2.4E-04	3.7E-04	2.0E-04	3.7E-04	2.0E-04	3.1E-04	2.0E-04	3.1E-04	2.0E-04	3.1E-04	2.0E-04	3.1E-04	2.0E-04	3.1E-04	2.0E-04	3.1E-04				
V	1.2E-04	1.9E-04	7.4E-05	1.1E-04	9.0E-05	1.4E-04	7.7E-05	1.4E-04	7.7E-05	1.2E-04	1.2E-04	1.2E-04	1.2E-04	1.2E-04	1.2E-04	1.2E-04	1.2E-04	1.2E-04	1.2E-04	1.2E-04				
Sr	3.5E-05	9.0E-08	7.4E-06	1.9E-08	1.1E-07	2.9E-08	1.7E-07	1.7E-05	1.7E-07	2.4E-08	1.4E-06	2.4E-08	1.4E-06	2.4E-08	1.4E-06	2.4E-08	1.4E-06	2.4E-08	1.4E-06	2.4E-08				
Total	4.5E-03	2.8E-07	8.8E-03	8.8E-06	7.7E-03	3.6E-07	1.2E-02	1.7E-07	3.4E-06	1.2E-02	1.0E-06	1.9E-02	1.0E-06	1.9E-02	1.0E-06	1.9E-02	1.0E-06	1.9E-02	1.0E-06	1.9E-02				

that as hand licking and biting toys and other objects, they are more vulnerable to dust exposure (Li et al. 2018).

The oral bioaccessibility of each metal was performed to obtain more accurate risk assessment of human exposure to trace metal concentrations in road dust (Li et al. 2017). Based on the bioaccessibility of the non-carcinogenic and carcinogenic trace metals in road dust, the HQ and CR for a child and an adult are listed in Table S6. Overall, all trace metals recorded HQ and HI values below the acceptable limit (< 1) where the highest HI value was recorded at RD for a child ($6.0E-02$) and the lowest was at LRT for an adult ($6.8E-04$). All carcinogenic elements recorded CR values below the acceptable limit ($1.0E-6$), indicating no significant risk from carcinogenic elements for both children and adults. When comparing HQ and CR values for the oral bioaccessibility fraction of road dust via the ingestion pathway, ingestion of road dust exhibits a much higher risk compared to the bioaccessibility fraction, for which highest risk was for As in road dust while it was for Zn and Sr in the bioaccessibility fraction. Zn recorded the highest HQ value for HT, LRT, and CM while Co had the highest for the GR and RD urban areas. For carcinogenic elements, Sr recorded the highest CR values for the HT, LRT, and CM locations while Pb did for the GR and RD locations. The highest risk was observed for a child which was about nine times and two times higher compared to an adult for non-carcinogenic and carcinogenic elements, respectively. The HQ and CR values for the bioaccessible fraction were suggested to be below and in range of the acceptable limits for children and adults but a much higher risk is posed to children compared to adults (Hu et al. 2011; Wang et al. 2016; Li et al. 2017).

Conclusion

Analysis of the trace metal and ion concentrations of road dust and the bioaccessible fraction was performed in five urban areas in Kuala Lumpur City. In comparison of the trace metal and ion concentrations with those found in other cities, low to medium levels were recorded. The highest metal concentration was recorded for Fe and the highest ion concentration was Ca^{2+} with overall averages of $12169 \pm 6507 \mu\text{g g}^{-1}$ and $3470 \pm 1693 \mu\text{g g}^{-1}$, respectively. Among the studied urban areas, the concentrations of trace metals and ions classified the sites in the order $LRT > HT > RD > CM > GR$ while trace metal concentrations in the bioaccessible fraction classified the sites in the sequence $LRT > CM > RD > GR > HT$. Arsenic exhibited the highest values for Igeo, PI, and EF compared to other trace metals, suggesting high levels of pollution and extreme contributions from anthropogenic sources. Major sources of road dust and the bioaccessible fraction were derived from vehicle and traffic activity and soil dust. The sequence of health risk pathways from road dust was ingestion $>$ dermal $>$ inhalation where

all non-carcinogenic and carcinogenic element values were recorded as below the acceptable limit and in the tolerable limit range except for arsenic. The bioaccessible fraction showed no significant risks from non-carcinogenic and carcinogenic elements via oral ingestion. Higher values of HQ and CR at the LRT site indicate that there were higher risks to the general population at LRT compared to other urban areas.

Acknowledgments Special thanks to Mrs. Azwani Alias for sampling assistance and Dr. Rose Norman for proof reading this manuscript.

Funding information Universiti Kebangsaan Malaysia and Ministry of Education provided research funding under research grant FRGS/1/2018/WAB05/UKM/01/1. This research is part of the project entitled Disaster Resilient Cities: Forecasting Local Level Climate Extremes and Physical Hazards for Kuala Lumpur supported by the Research and Innovation Bridges Programme of the Newton Ungku Omar Fund (XX-2017-002).

References

- Abbasi S, Keshavarzi B, Moore F, Turner A, Kelly FJ, Dominguez AO, Jaafarzadeh N (2019) Distribution and potential health impacts of microplastics and microrubbers in air and street dusts from Asaluyeh County. Iran Environ Pollut 244:153–164
- Al-Khashman OA (2004) Heavy metal distribution in dust, street dust and soils from the work place in Karak Industrial Estate, Jordan. Atmos Environ 38:6803–6812
- Al-Khashman OA (2007) Determination of metal accumulation in deposited street dusts in Amman, Jordan. Environ Geochem Health 29:1–10
- Ali MU, Liu G, Yousaf B, Abbas Q, Ullah H, Munir MAM, Fu B (2017) Pollution characteristics and human health risks of potentially (eco)toxic elements (PTEs) in road dust from metropolitan area of Hefei, China. Chemosphere 181:111–121
- Amil N, Latif MT, Khan MF, Mohamad M (2016) Seasonal variability of $PM_{2.5}$ composition and sources in the Klang Valley urban-industrial environment. Atmos Chem Phys 16:5357–5381
- Aminian MM, Baalausha M, Mousavi R, Aminian FM, Hosseini H, Heydariyan A (2017) The ecological risk, source identification, and pollution assessment of heavy metals in road dust: a case study in Rafsanjan, SE Iran. Environ Sci Pollut Res 25:13382–13395
- Amjadian K, Pirouei M, Mehr MR, Shakeri A, Rasool SK, Haji DI (2018) Contamination, health risk, mineralogical and morphological status of street dusts- case study: Erbil metropolis, Kurdistan region-Iraq. Environ Pollut 243(part B):1568–1578
- Arslan H (2001) Heavy metals in street dust in Bursa. Turkey J Trace Microprobe Tech 19:439–445
- Banerjee T, Murari V, Kumar M, Raju MP (2015) Source apportionment of airborne particulates through receptor modeling: Indian scenario. Atmos Res 164-165:167–187
- Behera SN, Sharma M (2012) Transformation of atmospheric ammonia and acid gases into components of $PM_{2.5}$: an environmental chamber study. Environ Sci Pollut Res 19:1187–1197
- Bhuiyan MA, Dampare SB, Islam MA, Suzuki S (2015) Source apportionment and pollution evaluation of heavy metals in water and sediments of Buriganga River, Bangladesh, using multivariate analysis and pollution evaluation indices. Environ Monit Assess 187:4075

- Cao Z, Yang Y, Lu J, Zhang C (2011) Atmospheric particle characterization, distribution, and deposition in Xi'an, Shaanxi Province, Central China. *Environ Pollut* 159:577–584
- Cayir A, Belivermis M, Kilic O, Coskun M (2012) Heavy metal and radionuclide levels in soil around Afsin-Elbistan coal-fired thermal power plants, Turkey. *Environ Earth Sci* 67:1183–1190
- Charlesworth S, Everett M, McCarthy R, Ordonez A, deMiguel EA (2003) A comparative study of heavy metal concentration and distribution in deposited street dusts in a large and a small urban area: Birmingham and Coventry, West Midlands UK. *Environ Int* 29:563–573
- Chen H, Lu X, Li LY, Gao T, Chang Y (2014) Metal contamination in campus dust of Xi'an China: A study based on multivariate statistics and spatial distribution. *Sci Total Environ* 484:27–35
- DBKL, 2018. Kuala Lumpur Structure Plan: Environment. <http://www.dbkl.gov.my/pskl2020/english/environment/index.htm> Dewan Bandaraya Kuala Lumpur, Kuala Lumpur Access on 25 December 2018
- Dehghani S, Moore F, Keshavarzi B, Hale BA (2017) Health risk implications of potentially toxic metals in street dust and surface soil of Tehran, Iran. *Ecotoxicol Environ Saf* 136:92–103
- DOE, 2018. Point source industries in Kuala Lumpur. Department of Environment, Kuala Lumpur, Kuala Lumpur (unpublished report)
- DOS, 2018. Federal Territory of Kuala Lumpur @ a glance. <https://www.dos.gov.my/v1/index> Department of Statistics Malaysia, Putrajaya Access on 25 December 2018
- Drahota P, Raus K, Rychliková E, Rohovec J (2017) Bioaccessibility of As, Cu, Pb, and Zn in mine waste, urban soil, and road dust in the historical mining village of Kaňk, Czech Republic. *Environ Geochem Health* 40:1495–1512
- Duong TTT, Lee B-K (2011) Determining contamination level of heavy metals in road dust from busy traffic areas with different characteristics. *J Environ Manag* 92:554–562
- Faiz Y, Tufail M, Javed MT, Chaudhry MM, Siddique N (2009) Road dust pollution of Cd, Cu, Ni, Pb and Zn along Islamabad expressway, Pakistan. *Microchem J* 92:186–192
- Gietl JK, Lawrence R, Thorpe AJ, Harrison RM (2010) Identification of brake wear particles and derivation of a quantitative tracer for brake dust at a major road. *Atmos Environ* 44:141–146
- Goix S, Uzu G, Oliva P, Barraza F, Calas A, Castet S, Point D, Masbou J, Duprey JL, Huayta C, Chincheros J, Gardon J (2016) Metal concentration and bioaccessibility in different particle sizes of dust and aerosols to refine metal exposure assessment. *J Hazard Mater* 317:552–562
- Gunawardana C, Goonetilleke A, Egodawatta P, Dawes L, Kokot S (2012) Source characterisation of road dust based on chemical and mineralogical composition. *Chemosphere* 87:163–170
- Han L, Zhuang G, Cheng S, Wang Y, Li J (2007) Characteristics of resuspended road dust and its impact on the atmospheric environment in Beijing. *Atmos Environ* 41:7485–7499
- Han NMIM, Latif MT, Othman M, Dominick D, Mohamad N, Juahir H, Tahir NM (2013) Composition of selected heavy metals in road dust from Kuala Lumpur city Centre. *Environ Earth Sci* 72:849–859
- Han X, Lu X, Qinggeletu, Wu Y (2017) Health risks and contamination levels of heavy metals in dusts from parks and squares of an industrial city in semi-arid area of China. *Int. J. Environ. Res. Public Health* 14:1–12
- Hu X, Zhang Y, Luo J, Wang T, Lian H, Ding Z (2011) Bioaccessibility and health risk of arsenic, mercury and other metals in urban street dusts from a mega-city, Nanjing. *China Environ Pollut* 159:1215–1221
- Jaradat QM, Momani KA, Jbarah AQ, Massadeh A (2004) Inorganic analysis of dust fall and office dust in an industrial area of Jordan. *Environ Res* 96:139–144
- Jayarathne A, Egodawatta P, Ayoko GA, Goonetilleke A (2017) Geochemical phase and particle size relationships of metals in urban road dust. *Environ Pollut* 230:218–226
- Jiang Y, Chao S, Liu J, Yang Y, Chen Y, Zhang A, Cao H (2016) Source apportionment and health risk assessment of heavy metals in soil for a township in Jiangsu Province, China. *Chemosphere* 168:1658–1668
- Jiries A (2001) Chemical composition of dew in Amman Jordan. *Atmos Res* 57:261–268
- Joshi UM, Vijayaraghavan K, Balasubramanian R (2009) Elemental composition of urban street dusts and their dissolution characteristics in various aqueous media. *Chemosphere* 77:526–533
- Kabadayi F, Cesur H (2010) Determination of Cu, Pb, Zn, Ni, Co, Cd, and Mn in road dusts of Samsun City. *Environ Monit Assess* 168:241–253
- Kastury F, Smith E, Juhasz AL (2017) A critical review of approaches and limitations of inhalation bioavailability and bioaccessibility of metal(loid)s from ambient particulate matter or dust. *Sci Total Environ* 574:1054–1074
- Khanal R, Furumai H, Nakajima F, Yoshimura C (2018) Carcinogenic profile, toxicity and source apportionment of polycyclic aromatic hydrocarbons accumulated from urban road dust in Tokyo, Japan. *Ecotoxicol Environ Saf* 165:440–449
- Khpalwak W, Jadoon WA, Abdel-dayem SM, Sakugawa H (2019) Polycyclic aromatic hydrocarbon in urban road dust, Afghanistan: implications for human health. *Chemosphere* 218:517–526
- Kong S, Ji Y, Lu B, Chen L, Han B, Li Z, Bai Z (2011) Characterization of PM10 source profiles for fugitive dust in Fushun—a city famous for coal. *Atmos Environ* 45:5351–5365
- Kurt-Karakus PB (2012) Determination of heavy metals in indoor dust from Istanbul, Turkey: Estimation of the health risk. *Environ Int* 50:47–55
- Leung AOW, Nurdan SD-Y, Cheung KC, Wong MH (2008) Heavy metals concentrations of surface dust from e-waste recycling and its human health implications in Southeast China. *Environ Sci Technol* 42:2674–2680
- Li H, Yu S, Li G, Deng H, Luo X (2011) Contamination and source differentiation of Pb in park soils along an urban-rural gradient in Shanghai. *Environ Pollut* 159:3536–3544
- Li HH, Chen LJ, Yu L, Guo ZB, Shan CQ, Lin JQ, Gu YG, Yang ZB, Yang YX, Shao JR, Zhu XM, Cheng Z (2017) Pollution characteristics and risk assessment of human exposure to oral bioaccessibility of heavy metals via urban street dusts from different functional areas in Chengdu, China. *Sci Total Environ* 586:1076–1084
- Li X, Poon CS, Liu PS (2001) Heavy metals contamination of urban soils and street dusts in Hong Kong. *Appl Geochem* 16:1361–1368
- Li X, Zhang M, Gao Y, Zhang Y, Zhang X, Yan X, Wang S, Yang R, Liu B, Yu H (2018) Urban street dust bound 24 potentially toxic metal/metalloids (PTMs) from Xining valley-city, NW China: spatial occurrences, sources and health risks. *Ecotoxicol Environ Saf* 162:474–487
- Liang J, Feng C, Zeng G, Gao X, Zhong M, Li X, Li X, He X, Fang Y (2017) Spatial distribution and source identification of heavy metals in surface soils in a typical coal mine city, Lianyuan, China. *Environ Pollut* 225:681–690
- Limbeck A, Handler M, Puls C, Zbiral J, Bauer H, Puxbaum H (2009) Impact of mineral components and selected trace metals on ambient PM₁₀ concentrations. *Atmos Environ* 43:530–538
- Liu Y, Ma J, Yan H, Ren Y, Wang B, Lin C, Liu X (2016) Bioaccessibility and health risk assessment of arsenic in soil and indoor dust in rural and urban areas of Hubei province, China. *Ecotoxicol Environ Saf* 126:14–22. <https://doi.org/10.1016/j.ecoenv.2015.11.037>
- Liu B, Wu J, Zhang J, Wang L, Yang J, Liang D, Dai Q, Bi X, Feng Y, Zhang Y, Zhang Q (2017) Characterization and source apportionment of PM_{2.5} based on error estimation from EPA PMF 5.0 model at a medium city in China. *Environ Pollut* 222:10–22
- Liu E, Yan T, Birch G, Zhu Y (2014) Pollution and health risk of potentially toxic metals in urban road dust in Nanjing, a mega-city of China. *Sci Total Environ* 476–477:522–531

- Liu M, Cheng SB, Ou DN, Hou LJ, Gao L, Wang LL, Xie YS, Yang Y, Xu SY (2007) Characterization, identification of road dust PAHs in Central Shanghai areas, China. *Atmos Environ* 41:8785–8795
- Lu X, Zhang X, Li LY, Chen H (2018) Assessment of metals pollution and health risk in dust from nursery schools in Xi'an, China. *Environ Res* 128:27–34
- Luo X, Yu S, Zhu Y, Li X (2012) Trace metal contamination in urban soils of China. *Sci Total Environ* 421–422:17–30
- Mathee A, Kootbodien T, Kapwata T, Naicker N (2018) Concentration of arsenic and lead in residential garden soil from four Johannesburg neighborhoods. *Environ Res* 167:524–527
- McCartney M, Davidson CM, Howe SE, Keating GE (2000) Temporal changes in the distribution of natural radionuclides along the Cumbrian coast following the reduction of discharges from a phosphoric acid production plant. *J Environ Radioact* 49:279–291
- McKenzie ER, Wong CM, Green PG, Kayhanian M, Young TM (2008) Size depended elemental composition of road-associated particles. *Sci Total Environ* 398:145–153
- Men C, Liu R, Xu F, Wang Q, Guo L, Shen Z (2018) Pollution characteristics, risk assessment, and source apportionment of heavy metals in road dust in Beijing, China. *Sci Total Environ* 612:138–147
- Morawska L, Ristovski Z, Jayaratne ER, Keogh DU, Ling X (2008) Ambient nano and ultrafine particles from motor vehicle emissions: characteristics, ambient processing and implications on human exposure. *Atmos Environ* 42:8113–8138
- Okorie A, Entwistle J, Dean JR (2012) Estimation of daily intake of potentially toxic elements from urban street dust and the role of oral bioaccessibility testing. *Chemosphere* 86:460–467
- Othman M, Latif MT, Matsumi Y (2019) The exposure of children to PM_{2.5} and dust in indoor and outdoor school classrooms in Kuala Lumpur city Centre. *Ecotoxicol Environ Saf* 170:739–749
- Padoan E, Romè C, Ajmone-Marsan F (2017) Bioaccessibility and size distribution of metals in road dust and roadside soils along a peri-urban transect. *Sci Total Environ* 601–602:89–98
- Patinha C, Duraes N, Sausa P, Dias AC, Reis AP, Noack Y, da Sila EF (2015) Assessment of the influence of traffic-related particles in urban dust using sequential selective extraction and oral bioaccessibility test. *Environ Geochem Health* 37:707–724
- Qing YM, Turpin BJ, Jong HL, Polidori A, Weisel CP, Morandi M, Colome S, Zhang J, Stock T, Winer A (2007) How does infiltration behavior modify the composition of ambient PM 2.5 in indoor spaces? An analysis of RIOPA data. *Environ Sci Technol* 41:7315–7321
- Rahman SA, Hamzah MS, Wood AK, Elias MS, Salim NAA, Sanuri E (2011) Sources apportionment of fine and coarse aerosol in Klang Valley, Kuala Lumpur using positive matrix factorization. *Atmos Pollut Res* 2:197–206
- Ramírez O, de la Campa AMS, Amato F, Moreno T, Silva LF, de la Rosa JD (2018) Physicochemical characterization and sources of the thoracic fraction of road dust in a Latin American megacity. *Sci Total Environ* 652:434–446
- Rasmussen PE, Beauchemin S, Nugent M, Dugandzic R, Lanouette M, Chenier M (2008) Influence of matrix composition on the bioaccessibility of copper, zinc, and nickel in urban residential dust and soil. *Hum Ecol Risk Assess* 14:351–371
- Rastmanesh F, Mousavi M, Zarasvandi A, Edraki M (2017) Investigation of elemental enrichment and ecological risk assessment of surface soils in two industrial port cities, Southwest Iran. *Environ Earth Sci* 76:1–13
- Rodrigues JLG, Bandeira MJ, Araújo CFS, dos Santos NR, Anjos ALS, Koin NL, Pereira LC, Oliveira SSP, Mergler D, Menezes-Filho JA (2018) Manganese and lead levels in settled dust in elementary schools are correlated with biomarkers of exposure in school-aged children. *Environ Pollut* 236:1004–1013
- Shi D, Lu X (2018) Accumulation degree and source apportionment of trace metals in smaller than 63 μm road dust from the areas with different land uses: a case study of Xi'an, China. *Sci Total Environ* 636:1211–1218
- Shi G, Chen Z, Bi C, Wang L, Teng J, Li Y, Xu S (2011) A comparative study of health risk of potentially toxic metals in urban and suburban road dust in the most populated city of China. *Atmos Environ* 45:764–771
- Shi G, Chen Z, Xu S, Zhang J, Wang L, Bi C, Teng J (2008) Potentially toxic metal contamination of urban soils and roadside dust in Shanghai, China. *Environ Pollut* 156:251–260
- Sulong NA, Latif MT, Khan MF, Amil N, Ashfold MJ, Wahab MIA, Chan KM, Sahani M (2017) Source apportionment and health risk assessment among specific age groups during haze and non-haze episodes in Kuala Lumpur, Malaysia. *Sci Total Environ* 601–602:556–570
- Tang Z, Chai M, Cheng J, Jin J, Yang Y, Nie Z, Huang Q, Li Y (2017) Contamination and health risks of heavy metals in street dust from a coal-mining city in eastern China. *Ecotoxicol Environ Saf* 138:83–91
- Taylor SR, McLennan SM (1985) The continental crust: its composition and evolution. Blackwell, Oxford
- Tian S, Liang T, Li K, Wang L (2018) Source and path identification of metals pollution in a mining area by PMF and rare earth element patterns in road dust. *Sci Total Environ* 633:958–966
- Urrutia-Goyes R, Hernandez N, Carrillo-Gamboa O, Nigam KDP, Ornelas-Soto N (2018) Street dust from a heavily-populated and industrialized city: evaluation of spatial distribution, origins, pollution, ecological risks and human health repercussions. *Ecotoxicol Environ Saf* 159:198–204
- USEPA, 2010a. Regional screening level. Available online at <http://www.epa.gov/region9/superfund/prg/index.html>. Accessed 12 February 2019
- USEPA (2010b) Risk assessment guidance for superfund volume 1, human health evaluation manual (part a). Office of Emergency and Remedial Response. United States Environmental Protection Agency, Washington
- USEPA, 2017. Standard operating procedure for an in vitro bioaccessibility assay for Lead and arsenic in soil. OLEM 9200.2-164. United States Environmental Protection Agency, Washington
- Valido IH, Padoan E, Moreno T, Querol X, Font O, Amato F (2018) Physico-chemical characterization of playground sand dust, inhalable and bioaccessible fractions. *Chemosphere* 190:454–462
- Wang J, Li S, Cui X, Li H, Qian X, Wang C, Sun Y (2016) Bioaccessibility, sources and health risk assessment of trace metals in urban park dust in Nanjing, Southeast China. *Ecotoxicol Environ Saf* 128:161–170
- Xie R K, Seip H M, Liu L, Zhang D S (2009) Characterization of individual airborne particles in Taiyuan City, China. *Air Qual Atmos Health* 2 (3):123–131. <https://doi.org/10.1007/s11869-009-0039-x>
- Yu B, Wang Y, Zhou Q (2014) Human health risk assessment based on toxicity characteristic leaching procedure and simple bioaccessibility extraction test of toxic metals in urban street dust of Tianjin, China. *PLoS One* 9:1–9
- Yu W, Liu R, Xu F, Men C, Shen Z (2016) Identifications and seasonal variations of sources of polycyclic aromatic hydrocarbons (PAHs) in the Yangtze River estuary, China. *Mar Pollut Bull* 104:347–354
- Zhao P, Feng Y, Zhu T, Wu J (2006) Characterizations of resuspended dust in six cities of North China. *Atmos Environ* 40:5807–5814
- Zheng N, Liu J, Wang Q, Liang Z (2010) Health risk assessment of heavy metals exposure to street dust in the zinc smelting district, Northeast of China. *Environ Geochem Health* 35:726–733